THE INTERNATIONAL JOURNAL OF SCIENCE & TECHNOLEDGE

Assessing the Potential of Image Segmentation on Google Earth Images for Carbon Estimation across Rubber Plantations of Different Ages

Ekow Nyamekye Tawiah
Alumni, Faculty of Geo-Information Science & Earth Observation (ITC),
University of Twente, Netherlands
Ing. George Ashiagbor
Research Fellow, Department of Wildlife & Range Management, College of Agriculture and Natural Resources, Kwame Nkrumah University of Science & Technology, Ghana
Ir. Louise van Leeuwen
Lecturer, Faculty of Geo-Information Science & Earth Observation (ITC),
Institution name: University of Twente, Netherlands
Dr. Winston Adams Asante
Lecturer, Department of Silviculture & Forest Management, College of Agriculture and Natural Resources, Kwame Nkrumah University of Science & Technology, Ghana
Jefferson Okojie
Alumni, Faculty of Geo-Information Science & Earth Observation (ITC),
University of Twente, Netherlands

Abstract:
The evolution of remote sensing technologies has improved scientific study and research. The often high cost of satellite images has led to research into alternative remotely sensed data for various analysis. Google earth data being cheap and readily available has been employed in many analyses including textural analysis with positive results. The application of OBIA to google earth image was employed in this study to assess the predictive ability of rubber tree diameter at breast height towards carbon modelling. Out of a total of 190 manually delineated tree crowns, 102 trees were found to have a 1 to 1 matching with segmented crowns on the Google Earth images were used. For the whole study area over-segmentation value was 0.43 (43% error) and the under-segmentation was 0.32 (32% error) with the D-Value computed as 0.38 (38% error) which means that the segmentation accuracy is 62%. Models developed from the segmentation process and field data were linear, quadratic and cubic models with R^2 of 0.014, 0.137 and 0.139 respectively. Primarily, these poor R^2 values are due to the fact that Google earth images have poor spectral values, red and infrared portions are absent which affect the clear crown detection of the tree canopies. The tree canopies are equally highly clustered, therefore with poor spectral values individual tree detection using OBIA procedure achieves very little success in the diameter at breast height prediction.

Keywords: *Carbon pool, latex, aboveground, belowground, rubber, carbon, segmentation*

1. Introduction

Although native to the Amazon Basin area, the rubber (Hevea brasiliensis) plantations have successfully been introduced to other tropical countries across the world (Venkatachalam, Geetha, Sangeetha, & Thulaseedharan, 2013). There has been massive expansion of rubber plantations in the tropical and sub-tropical regions of the world over the past 50 years (Chen et al., 2016). This rapid development of rubber plantations is recorded in Southeast-Asia and Africa with an estimated total area of 10 million hectares (M ha) out of the estimated 4 billion hectares (B ha) for total world forests (FAO, 2010). Thus, rubber plantations constitute a quarter of total world forest cover since they are considered as planted forests (Egbe, 2012).

Increasing estimates of area coverage for rubber plantations require an insight into environmental impacts in relation to the amount of carbon it sequesters as a carbon pool (Nizami et al., 2014). For plant growth and development, rubber plantations like every other vegetation sequester carbon owing to accumulations in the below ground biomass (BGB), soil organic carbon (SOC), latex production and most significantly above ground biomass (AGB) (Blagodatsky, Xu, & Cadisch, 2016). The sequestration abilities of rubber thrive on the age, management and environmental (climatic and topographical) factors.

Remote Sensing approach of using satellite imagery to extract the biophysical properties of vegetation in order to calculate biomass and subsequently carbon has gain notoriety (Lu et al., 2014). To validate the accuracy of remotely

sensed data, it is complemented with field data collected by means of sampled biophysical properties. This technology may employ active sensors or passive sensors which are dependent on detection of reflected solar radiation from the earth surface (mostly optical sensors) (Lu, 2006). Remote sensing approach presents a faster way of data collection over vast areas and is less labour intensive compared to the destructive method of tree felling. Optical imagery with Very High Resolution (VHR) of less than 5 m provide fine details which help to extract tree parameters such as the crown projected area (CPA) which forms a basis for extracting tree parameters for biomass estimation (Karna et al., 2015).

Image segmentation method can be used to extract tree biophysical information from VHR or object-based image analysis (OBIA) aids in segregating image objects into distinct non overlapping elements by considering spectral, shape, textural, pattern including the location (Bakx et al., 2013). This combination of VHR imagery and segmentation based on objects proves useful for biomass and carbon estimation since it gives biophysical details for individual trees(Hay, Castilla, Wulder, & Ruiz, 2005).

Carbon estimation of rubber plantations for vast areas could be tedious and cumbersome given time and financial resources. The measurement of tree biophysical characteristics such as Diameter at Breast Height (DBH) as an input for allometric equations to estimate carbon from rubber plantations can be done indirectly using segmented crowns from Very High Resolution (VHR) remotely sensed data. The availability of free Very High Resolution (VHR) Imagery from Google Earth could serve as a useful indirect method for carbon estimation. The application of Google EarthImagery for the extraction of rubber tree crowns for carbon estimation has not yet been well explored.

Therefore, the potential of using Google Earth Images to estimate aboveground and belowground carbon across different ages of rubber plantations is explored by this study.

2. Materials and Methods

2.1. Study Area

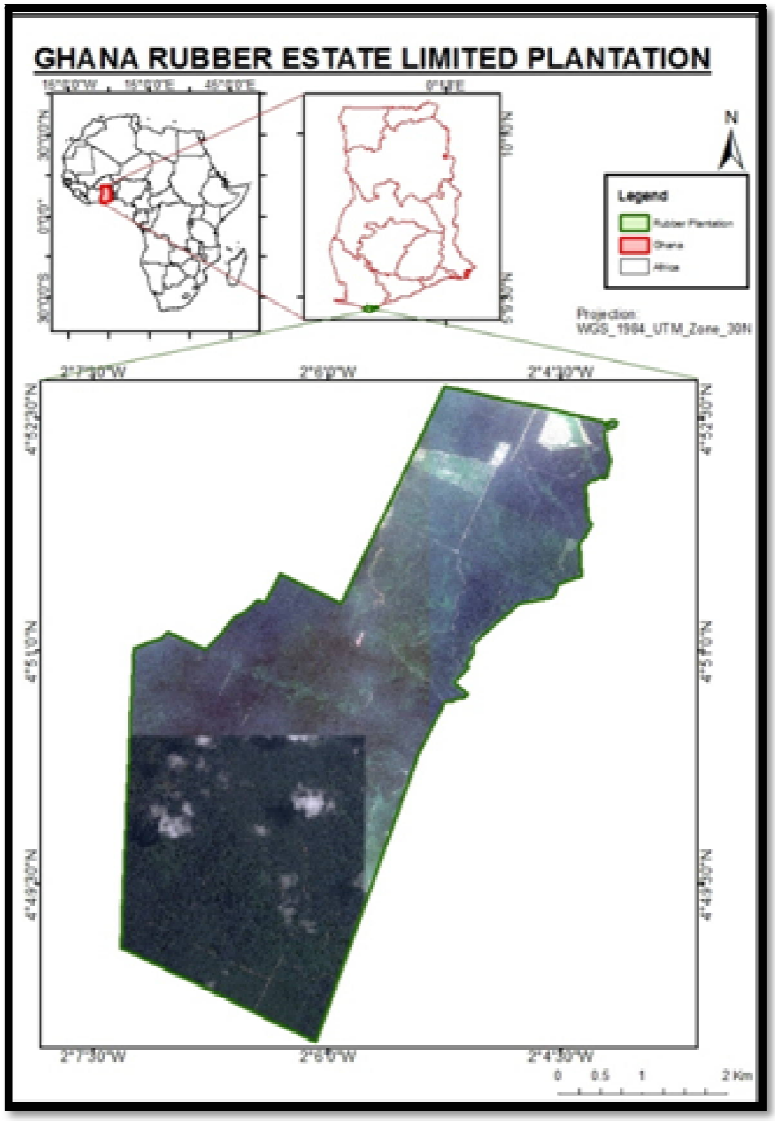

Figure 1: Study Area

2.2. Data

Stratified random sampling procedure was used in this study since the rubber plantations are of different ages and are homogenous at the age class level(Omair, 2014). This method has been found to be useful for rubber plantations related studies for estimating carbon and biomass (Wauters et al., 2008; Charoenjit et al., 2015).The different age classes in this study area are 22, 21, 20, 19, 17, 12, 11 and 9 with different tree densities in each plot. 25 sample points (Figure 2) were randomly selected across the different age classes for the study area.

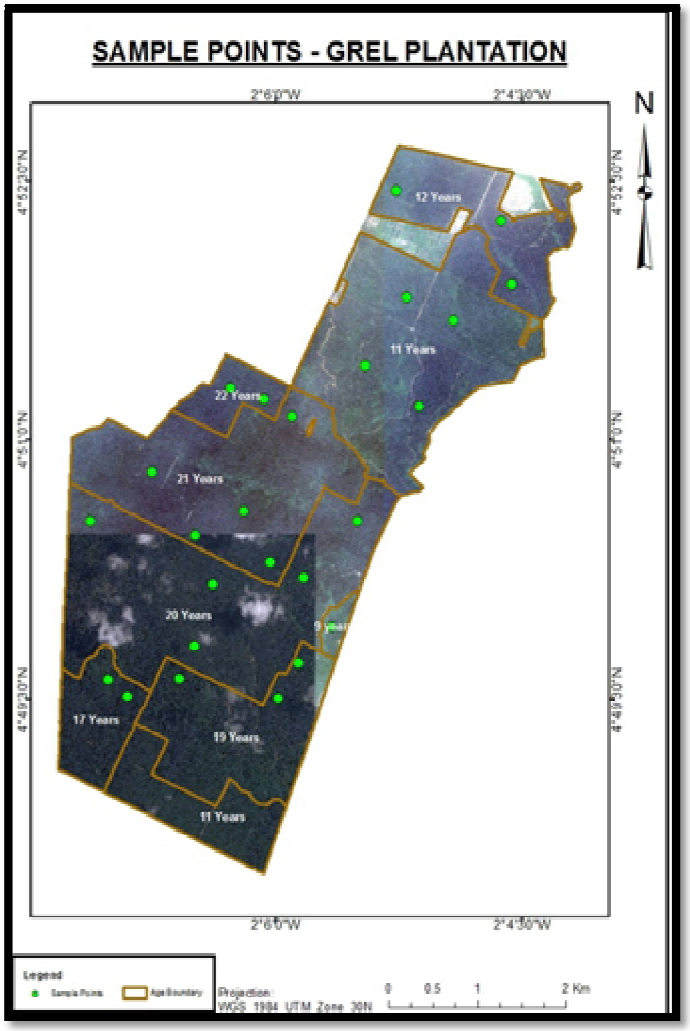

Figure 2: Sample Points

Global Positioning Service (GPS) devices were preloaded with coordinates of all the sample points for the field points data collection. Circular plots of 500m^2 were made per sample point. Measurements of diameter at breast height of 170cm (DBH_{170}) and CPA of each tree within the plots were the parameters measured.

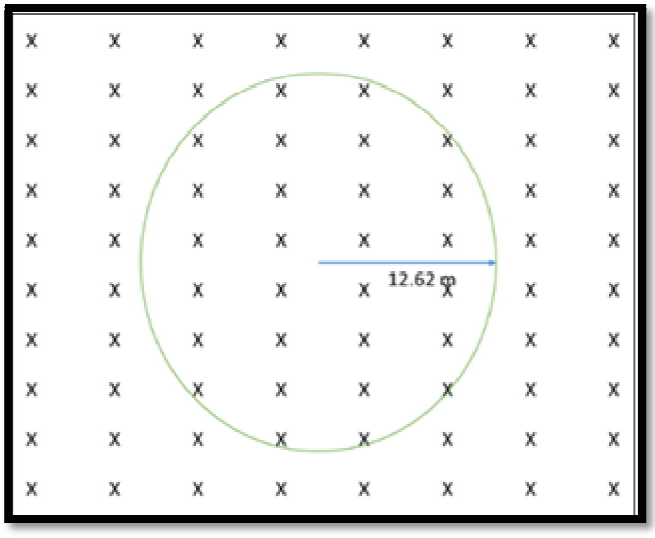

Figure 1: 500 m^2 Circular Plot

2.2.1. Image Segmentation Process

The estimation of scale parameter (ESP) tool was loaded into the eCognition software together with the Image for the estimation of suitable scale for the segmentation process. Figure 4 below shows the threshold at which the Google Earth Imagery could be objectively segmented. The first image shows the whole trend and the second image zooms in to further see the value where the ROC line peaks. A scale factor of 20 was chosen for the segmentation.

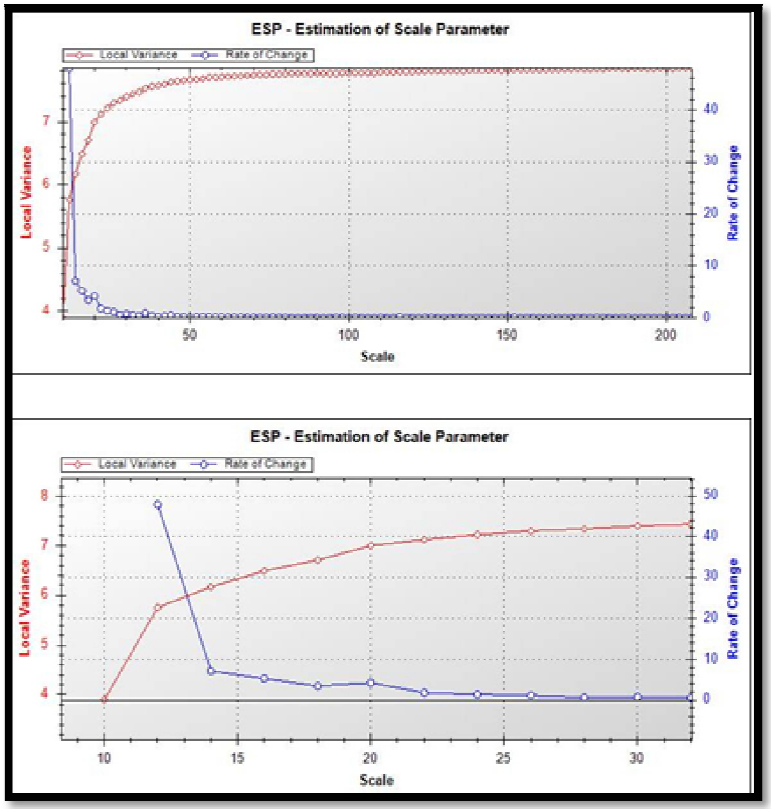

Figure 2: ROC-LV for ESP

The Google Earth image was digitised into the different age classes of 22, 21, 20, 19, 17, 12, 11, and 9-year-old stands. The digitised classes were used to extract each age class from the Google Earth image for the segmentation process to be conducted on age by age basis. Manual delineation of the crowns of the individual trees observed in the plots and identified on the Google Earth image was conducted. The manual delineation of individual crowns was also performed with the aim of conducting an accuracy assessment to validate the segmented image objects.

Although there exists other segmentation algorithms, the multi-resolution segmentation algorithm is widely used to successfully obtain image object segments (Hay et al., 2005; Rejaur Rahman & Saha, 2008). The scale parameter used for the multi-resolution segmentation was 20 with shape and compactness set at 0.5 each. This resulted in the generation of image object segments, however, not all the segments were proper, therefore the need to refine the segments.

Due to the mosaic king of several images to form the Google Earth imagery, there were shadows and clouds in the imagery which were masked using the brightness values. These shadows and clouds were merged separately and classified as such and excluded from subsequent analysis.

This algorithm was used to refine the image segments to split large crowns and clustered crowns into separate tree. The factor used here was 10 pixels since maximum field observation of Tree crown was observed at 3m and the Google Earth Image has a resolution of 30cm.

The results of the watershed transformation did not come out as the desirable (rounded) segments, hence the need for the morphology algorithm to be run. The Open Image object parameter was adopted to remove pixels which were separated from the segmented objects. A circular mask was also created for defining the size and shape to bring about the almost circular shape of tree crowns.

Undesirable image objects were removed after the watershed transformation and morphological operations. Image objects which were unwanted segmentation such as tiny and elongated objects were removed on the basis of roundness, area of pixel attributes. The rule set which refers to the command processes employed in the segmentation process is as shown below in Figure 5.

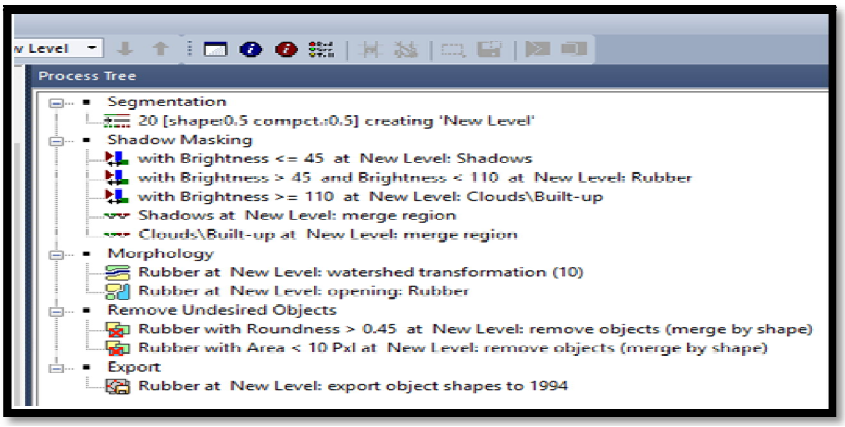

Figure 5: Segmentation Rule Set
Validation of Segmentation

A combination of topological, geometric and visual techniques was employed to assess the accuracy of the segments created using manually digitized reference polygons of the crowns of the rubber trees. This was carried out by considering the extent to which reference polygons and image object segments match each other in terms of position, size and shape by at least 50%. The overall accuracy of the segmentation results was determined using the segmentation goodness of fit, the "D" in Equation 1. This was made possible by first computing over-segmentation using Equations 2 and under-segmentation using Equation 3. The Figure 6 below shows the matching conditions as expressed by (a) over 50% match (b) same shape and size of segments with reference objects but for differences in position; (c) and (d) segments and reference objects may be of match with respect to position but not of same spatial extent. Common areas of overlap are indicated in red whereas areas of differences are identifiable in blue and green respectively.

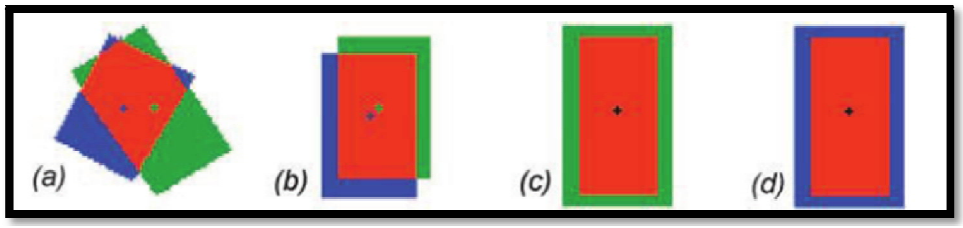

Figure 6: Matched Cases of Extracted Objects
Source: (Zhan, Molenaar, Tempfli & Shi, 2005)

2.2.2. Model Development

To analyse the relationship between then Google Earth derived CPA and DBH for the purposes of carbon modelling, regression analysis was conducted. A non-linear relationship between the CPA which was the dependent variable and the DBH as an independent variable was established. This was to help evaluate the extent to which the CPA could predict DBH accurately for the purposes of carbon modelling using the OBIA procedure.

Trees with one to one matching in terms of those identified on the field and those obtained from the segmentation process of the Google Earth imagery were used. From the identified 102 trees 70 trees were used for the model development and the remained 32 were used for the validation. The Root Mean Square Error (RMSE) was computed by comparing the predicted values derived from the segmentation process against the observed values from the field shown by Equation 4.

$$D_{ij} = \sqrt{\frac{Over-Segmentation_{ij}^2 + Under-Segmentation_{ij}^2}{2}} \quad \text{Segmentation Goodness..... (1)}$$

$$Over-Segmentation_{ij} = 1 - \frac{area(x_i \cap y_j)}{Area(X_i)}, y_i \in Y_i^* \quad \text{Over-Segmentation..... (2)}$$

$$Under-Segmentation_{ij} = 1 - \frac{area(x_i \cap y_j)}{Area(Y_i)}, \quad \text{Under-Segmentation..... (3)}$$

$$y_i \in Y_i^* \quad \text{Root Mean Square Error..... (4)}$$

3. Results

3.1. Multi-Resolution Segmentation

Results of the multi-resolution segmentation, cloud and shadow masking, morphology and watershed transformation is shown in Figure 7. The scale parameter set was 20 and 0.5 for both shape and compactness as obtained from the ESP tool.

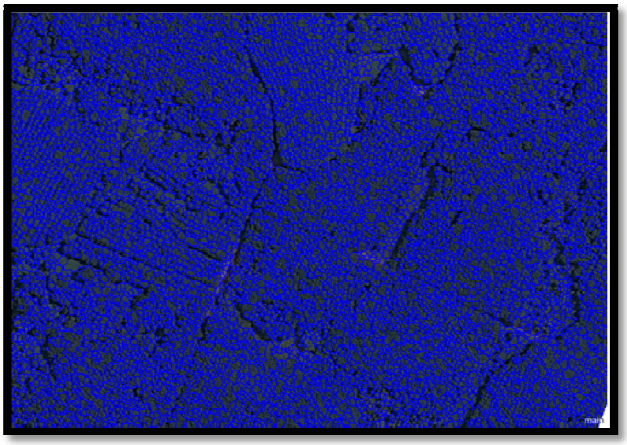

Figure 3: Tree Crown Delineation Using Multi-Resolution Segmentation

3.2. Accuracy Assessment

The segmentation accuracy was assessed using the goodness of fit "D" value computed from the results of over-segmentation and under-segmentation. Out of total of 190 manually delineated tree crowns, 102 trees were found to have a 1 to 1 matching with segmented crowns on the Google Earth images were used. For the whole study area over-segmentation value was 0.43 (43% error) and the under-segmentation was 0.32 (32% error) with the D-Value computed as 0.38 (38% error) which means that the segmentation accuracy is 62%. Table 1 below a summary of the accuracy assessment. This also summary shows that over-segmentation is greater than under-segmentation.

	Total Reference Polygons	Total 1:1 Match	Over-Segmentation	Under-Segmentation	D-value
1:1	190	102			
Goodness of fit			0.43	0.32	0.38
Total accuracy		53.70%			62%

Table 1: Segmentation accuracy

Figure 8 shows an overlay of reference polygons for segmentation accuracy assessment in red polygons on top of the and Google Earth image.

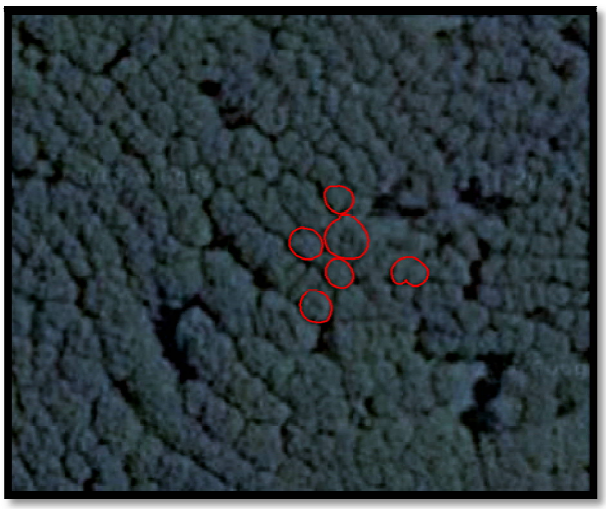

Figure 4: Shows an Overlay of the Manual Crown Delineation Relationship between Google Earth Derived Canopy Projection Area and Diameter at Breast Height

To determine the extent to which DBH values can be predicted using Google Earth derived image object segments, a non-linear relationship between the Google Earth derived CPA and DBH was established. The models were developed using the trees spotted in the field and the trees spotted in the image. Figure 9 shows linear and non-linear relationships that were established between the two variables (DBH as dependent variable and Google Earth derived CPA as independent variable).

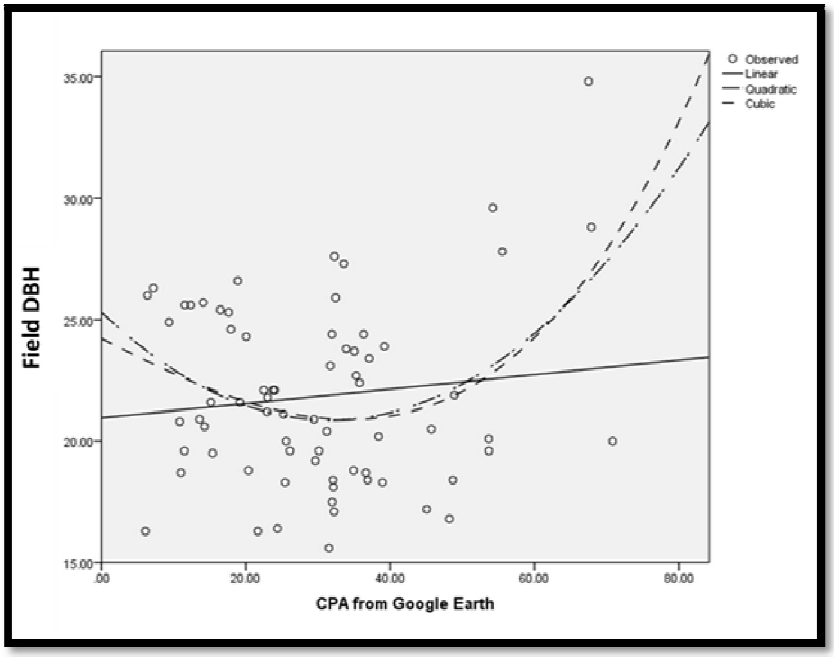

Figure 9: Relationship between DBH from Field Data and Google Earth Derived CPA

The linear, quadratic and cubic models were evaluated and reported in Table 2. From the models developed, the quadratic model had an RMSE value 0.15 and a mean absolute percentage error (MAPE) of 0.159. The cubic model reported a higher RMSE value of 0.28 and a MAPE of 0.161 with the linear model presenting the highest RMSE value of 1.19 and a MAPE of 0.421. The linear, quadratic and cubic models recorded correlation co-efficient values of 0.119, 0.370 and 0.373 and R^2 values of 0.014, 0.137 and 0.139, respectively indicating a weak correction between variables.

Model Type	r	R^2	RMSE	MAPE	p-value
Linear	0.119	0.014	1.190	0.421	0.327
Quadratic	0.370	0.137	0.150	0.159	0.007
Cubic	0.373	0.139	0.280	0.161	0.019

Table 2: Models for estimating DBH

4. Discussions

Segmentation results were based on objects that exhibited 50% one to one matching between image object segments and manually delineated crowns (Zhan et al., 2005). The segmentation process for the Google Earth Imagery yielded 43% over-segmentation error for the and an under-segmentation error of 32% with overall Goodness of fit at 62%. The segmentation accuracy does not differ much from that of Bautista (2012) who obtained 62% accuracy in segmentation of optical Geo-eye Image although the objects he was looking at were primary forests with larger tree crown. The author obtained over segmentation error of 48% of which was higher than in the case of the Google Earth Imagery segments although under segmentation error was lower than the Google Earth Imagery segments at 23%. Accordingly, Karna et al., (2015) obtained segmentation accuracy of 67% on WorldView-2 which is equally not too different from the overall segmentation accuracy obtained for the Google Earth Imagery segmentation from process.

However, there are differences in the correlation coefficients and the coefficients of determination in the models developed in spite of the similar segmentation accuracies. The results of the modelling from the Google Earth Imagery segmentation indicated that none of the three models (linear, quadratic, and cubic) could strongly predict DBH. The correlation coefficients were weak as the best correlation coefficient was exhibited by the quadratic model which had an r value of 0.37 and the coefficients of determination at best was 0.137. Karna et al., (2015) and Bautista (2012) reported an r of 0.871 and 0.72 and an R^2 of 0.759 and 0.41 showing stronger relationships between the various variables in their models.

The weak correlation between the DBH and the Google Earth imagery derived CPA can be attributed to the highly dense nature of the rubber tree crowns coupled with the poor spectral resolution to clearly delineate the rubber tree crowns automatically (Hu et al., 2013). Vegetation exhibit higher reflectance in the near infrared portion which is absent

from the Google Earth Imagery therefore dense crowns of the same age and similar characteristics could not be clearly distinguished from the google image (Li & Fox, 2012).

According to Bluman (2012), a correlation coefficient of 1 and -1 indicates a strong correlation hence as the correlation values decreases towards 0, a weak correlational effect exists among variables under study. The author further posits that coefficient of determination describes the amount of variation in predicted variables that models can explain. In this context the models developed from the Google Earth derived CPA could not adequately account for more than 80% of the variation in the DBH. Therefore, based on this study, Google Earth derived segments cannot be used to predict DBH of rubber plantations with dense canopy cover.

5. Conclusion

There is no relationship between Google Earth derived image object segments and field measured diameter at breast height. As the linear, quadratic and cubic models could only account for 1.4%, 13.7% and 13.9% of the variation in the diameter at breast height.

6. Recommendations

The multi-resolution segmentation process performed on the Google Earth could not lead to the development of accurate models to establish a relationship between the image object segments and field collected DBH. Further exploration should be conducted to focus on building models for each age compartment found within rubber plantations landscape, as well as alternative segmentation algorithms that can perform better than the multi-resolution segmentation algorithm.

7. References

i. Andrew E. Egbe. (2012). Simulation of the impacts of three management regimes on carbon sinks in rubber and oil palm plantation ecosystems of South- Western Cameroon. Journal of Ecology and the Natural Environment, 4(6), 154–162. https://doi.org/10.5897/JENE11.146

ii. Bakx, W., Janssen, L., Schetselaar, E., Tempfli, K., Tolpekin, V., & Westinga, E. (2013). Chapter 06 - Image Analysis. In The core of GIScience a process based approach. (pp. 205–225). Enschede: Faculty of Geo-Information Science and Earth Observation (ITC) of the University of Twente. Retrieved from https://issuu.com/itc-utwente/docs/corebook2013_06_imageanalysis

iii. Bautista, L. A. A. (2012). Biomass Carbon Estimation and Mapping in the Subtropical Forest of Chitwan, Nepal : a comparison between VHR geo-eye satellite images and airborne LIDAR data. University of Twente, Faculty of Geo-Information and Earth Observation (ITC). (MSc. Thesis). Retrieved from http://www.itc.nl/library/papers_2012/msc/nrm/lopezbautista.pdf

iv. Blagodatsky, S., Xu, J., & Cadisch, G. (2016). Carbon balance of rubber (Hevea brasiliensis) plantations: A review of uncertainties at plot, landscape and production level. Agriculture, Ecosystems and Environment, 221, 8–19. https://doi.org/10.1016/j.agee.2016.01.025

v. Bluman, A. G. (2012). Elementary Statistics A Step by Step Approach. McGraw Hill (8th edn). New York, NY: McGraw-Hill. https://doi.org/10.1007/s13398-014-0173-7.2

vi. Charoenjit, K., Zuddas, P., Allemand, P., Pattanakiat, S., & Pachana, K. (2015, March 19). Estimation of biomass and carbon stock in Para rubber plantations using object-based classification from Thaichote satellite data in Eastern Thailand. Journal of Applied Remote Sensing. Universit´e Pierre et Marie Curie. Paris. https://doi.org/10.1117/1.JRS.9.096072

vii. Chen, B., Li, X., Xiao, X., Zhao, B., Dong, J., Kou, W., ... Xie, G. (2016). Mapping tropical forests and deciduous rubber plantations in Hainan Island, China by integrating PALSAR 25-m and multi-temporal Landsat images. International Journal of Applied Earth Observation and Geoinformation, 50, 117–130. https://doi.org/10.1016/j.jag.2016.03.011

viii. Hay, G. J., Castilla, G., Wulder, M. A., & Ruiz, J. R. (2005). An automated object-based approach for the multiscale image segmentation of forest scenes. International Journal of Applied Earth Observation and Geoinformation, 7(4), 339–359. https://doi.org/10.1016/j.jag.2005.06.005

ix. Hu, Q., Wu, W., Xia, T., Yu, Q., Yang, P., Li, Z., & Song, Q. (2013). Exploring the use of google earth imagery and object-based methods in land use/cover mapping. Remote Sensing, 5(11), 6026–6042. https://doi.org/10.3390/rs5116026

x. Karna, Y. K., Hussin, Y. A., Gilani, H., Bronsveld, M. C., Murthy, M. S. R., Qamer, F. M., ... Baniya, C. B. (2015). Integration of WorldView-2 and airborne LiDAR data for tree species level carbon stock mapping in Kayar Khola watershed, Nepal. International Journal of Applied Earth Observation and Geoinformation, 38, 280–291. https://doi.org/10.1016/j.jag.2015.01.011

xi. Li, Z., & Fox, J. M. (2012). Mapping rubber tree growth in mainland Southeast Asia using time-series MODIS 250 m NDVI and statistical data. Applied Geography, 32(2), 420–432. https://doi.org/10.1016/j.apgeog.2011.06.018

xii. Lu, D. (2006). The potential and challenge of remote sensing-based biomass estimation. International Journal of Remote Sensing, 27(7), 1297–1328. https://doi.org/10.1080/01431160500486732

xiii. Lu, D., Chen, Q., Wang, G., Liu, L., Li, G., & Moran, E. (2014). A survey of remote sensing-based aboveground biomass estimation methods in forest ecosystems. International Journal of Digital Earth, 9(December), 1–43. https://doi.org/10.1080/17538947.2014.990526

xiv. Nizami, S. M., Yiping, Z., Liqing, S., Zhao, W., Zhang, X., & Wang, S. (2014). Managing carbon sinks in rubber (Hevea brasilensis) Plantation by changing rotation length in SW China. PLoS ONE, 9(12), 1–9. https://doi.org/10.1371/journal.pone.0115234

xv. Omair, A. (2014). Sample size estimation and sampling techniques for selecting a representative sample. Journal of Health Specialties, 2(4), 142. https://doi.org/10.4103/1658-600X.142783

xvi. Rejaur Rahman, M., & Saha, S. K. (2008). Multi-resolution segmentation for object-based classification and accuracy assessment of land use/land cover classification using remotely sensed data. Journal of the Indian Society of Remote Sensing, 36(2), 189–201. https://doi.org/10.1007/s12524-008-0020-4

xvii. Venkatachalam, P., Geetha, N., Sangeetha, P., & Thulaseedharan, A. (2013). Natural rubber producing plants : An overview. African Journal of Biotechnology, 12(12), 1297–1310. https://doi.org/10.5897/AJBX12.016

xviii. Wauters, J. B., Coudert, S., Grallien, E., Jonard, M., & Ponette, Q. (2008). Carbon stock in rubber tree plantations in Western Ghana and Mato Grosso (Brazil). Forest Ecology and Management, 255(7), 2347–2361. https://doi.org/10.1016/j.foreco.2007.12.038

xix. Zhan, Q., Molenaar, M., Tempfli, K., & Shi, W. (2005). Quality assessment for geo-spatial objects derived from remotely sensed data. International Journal of Remote Sensing, 26(14), 2953–2974. https://doi.org/10.1080/01431160500057764